ARTICLES

Separation of the Ultraviolet−Visible Spectra of the Redox States of Conducting Polymers by Simultaneous Use of Electron-Spin Resonance and Ultraviolet−Visible Spectroscopy

Andreas Neudeck, Andreas Petr, and Lothar Dunsch*

Institut für Festkörper-und Werkstofforschung Dresden, Institut für Festkörperforschung, Abteilung Elektrochemie und leitfähige Polymere, Helmholtzstrasse 20, D-01069 Dresden, Germany

Received: August 15, 1998; In Final Form: November 1, 1998

The electrochemical oxidation of polyaniline (PAni) films on gold electrodes is studied by simultaneous electron spin resonance (ESR) and UV−vis spectroelectrochemistry. The technique permits the separation of the superimposed UV−vis spectra of three redox states: the protonated reduced polyaniline chains, the deprotonated polaronic state, and the bipolaronic state. The separated UV−vis spectra as well as the potential dependence of each redox state concentration enables a more precise determination of the energy levels and the stability of paramagnetic species.

1. Introduction

The electrochemical oxidation of conducting polymers induces three different redox states. Starting from the reduced state A, most of the conducting polymers are oxidized in the first wave into different oxidation states B and C. The first state B is characterized by an unpaired delocalized spin, which was shown for a lot of different conducting polymers by in situ ESR spectroscopy.[1−3] It is nowadays described as the polaronic state B. The other redox state C gives no ESR signal. The characterization of the third redox state was mostly done by in situ UV−vis spectroscopy.[4,5] But the broad absorption bands of the spectra of the third oxidation state C are superimposed by those of the polaronic state B and of the reduced state A. These broad bands do not permit a separation of the spectra in a conventional way to get more information about the band energies.[6,7]

The third redox state C is often discussed as a bipolaronic state resulting from a second electron transfer from a polaronic segment B on the polymer chain to the electrode or by recombination of two polaronic states B on the chain yielding one reduced segment A and one bipolaronic segment C on the chain, considering the same extension of the bipolaronic segment as for the polaronic segment. Therefore, the electrochemical oxidation can be described as an EE mechanism that includes the disproportionation equilibrium

$$\begin{aligned} \mathrm{A} &\rightleftharpoons \mathrm{B} + \mathrm{e} \qquad E_1^\circ \\ \mathrm{B} &\rightleftharpoons \mathrm{C} + \mathrm{e} \qquad E_2^\circ \\ 2\mathrm{B} &\rightleftharpoons \mathrm{A} + \mathrm{C} \quad K_{\mathrm{disp}} = \mathrm{e}^{-F(E^0{}_2-E^0{}_1)/(RT)} = \mathrm{e}^{-F\Delta E^0/(RT)} \end{aligned} \tag{I}$$

where $E_1^\circ > E_2^\circ$. The single redox peak in the cyclic voltammogram seems to be due to "inverted" formal potential ($E_1^\circ > E_2^\circ$). The bipolaronic state C is energetically favored compared to the polaronic state B. Theoretical calculations for infinite polymer chains are in agreement with this explanation, but the extrapolation of the formal potentials of the corresponding oligomers to the conjugation length in the polymer does not result in an inversion of the formal potentials.

A single cyclovoltammetric wave with two products created simultaneously can also be described by a followup chemical equilibrium as the reversible dimerization determined for oligomers.[8−14]

$$\begin{aligned} \mathrm{A} &\rightleftharpoons \mathrm{B} + \mathrm{e} \qquad E_1^\circ \\ 2\mathrm{B} &\rightleftharpoons \mathrm{dimer} \qquad K_{\mathrm{dim}} \end{aligned} \tag{II}$$

In the case of a polymer film the dimerization reaction yields doubly charged segments on a polymer chain with a size twice as big as a polaronic segment. Such states are, for example, interchain bipolarons with a p or s bond between the polymer chains or simple bipolaronic states with a size that is 2 times bigger than that of a polaron.

On the other hand the redox peak might contain both processes I and II, depending on the location of the equilibrium and ΔE°.

In the case of conducting polymers such as polyaniline where the redox process includes protonation and deprotonation steps, the mechanism has to be written as

$$\begin{aligned} \mathrm{AH}^+ &\rightleftharpoons \mathrm{BH}^{\bullet 2+} + \mathrm{e} \qquad E_1^\circ, E_1^\circ > E_3^\circ \\ \mathrm{BH}^{\bullet 2+} &\rightleftharpoons \mathrm{B}^{\bullet +} + \mathrm{H}^+ \qquad K_{\mathrm{A}} \\ \mathrm{B}^{\bullet +} &\rightleftharpoons \mathrm{C}^{2+} + \mathrm{e} \qquad E_3^\circ \\ \text{net: } 2\mathrm{B}^+ &\rightleftharpoons \mathrm{A} + \mathrm{C}^{2+} \qquad K_{\mathrm{disp}} = \mathrm{e}^{-F(E^0{}_3-E^0{}_1)/(RT)} \\ \text{net: } 2\mathrm{B}^+ &\rightleftharpoons \mathrm{dimer}^{2+} \qquad K_{\mathrm{dimer}} \end{aligned} \tag{III}$$

Here, one considers that only the deprotonation after the first electron transfer occurs. Under these conditions the inversion is connected to the pK_{A} value of the deprotonation.[15−20] The

10.1021/jp983383k CCC: $18.00
Published on Web 01/23/1999

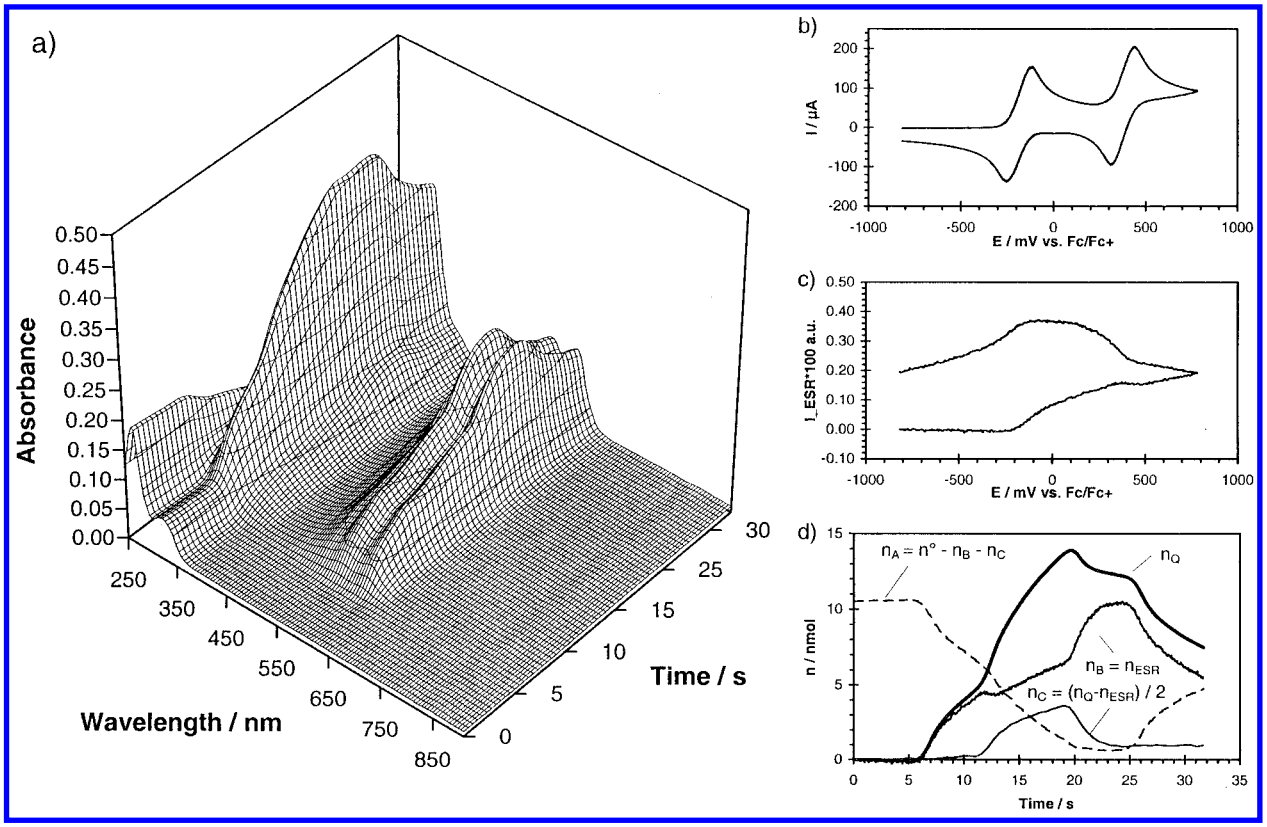

Figure 1. ESR UV−vis spectrocyclovoltammogram of 2 mM Wurster reagent solution in 0.1 M Bu_4NPF_6 on a laminated Au micromesh (1 mm × 3 mm) in a quartz glass flat cell with a slit width of 0.5 mm: (a) 61 UV−vis spectra recorded during the cyclovoltammetric scan; (b) in situ cyclovoltammetric curve recorded with a scan rate of 100 mV/s; (c) ESR intensity recorded at constant field with a modulation amplitude of 10 G; (d) resulting time dependence of the concentration of the three redox states after spectra separation (cf. Figure 2).

redox mechanism of the polymer chain can be treated as an ECE process.

To get precise data of the $\Delta G°$ values for the single steps of the process to compare the experimental results with calculations on polymer chains of finite and infinite length, it is necessary to determine the reaction mechanism. On the basis of this mechanism, it is possible to get the correct interpretation of the determined formal potentials. Cyclic voltammetry and spectrocyclovoltammetry using either UV−vis or ESR spectroscopy alone are insufficient for this purpose because of the superimposed UV−vis spectra and the independent detection of the species with the unpaired spin. Furthermore, the mechanism is superimposed by other processes as an exchange of counterions[21−27] and as a propagation of the conductive zone into the polymer layer.[28−37]

Detecting the amount of each oxidation state versus the potential/time scale of the experiment permits detailed information about the mechanism to distinguish among mechanisms I−III.

In several papers[6,7] UV−vis spectroscopy is used in electrochemical experiments to determine the band energies of the different oxidation states, but the separation of the superimposed spectra of the different oxidation states is mostly done qualitatively.[4,5] The present paper describes the way to get more information from the UV−vis spectroscopic data by simultaneous use of ESR spectroscopy and special data treatment.

2. Experimental Section

2.1. Equipment. The in situ ESR UV−vis spectrocyclovoltammetric measurements were controlled by a homemade program driving a potentiostat (PG285, HEKA-Elektronik, Lambrecht, Germany) by AD−DA plug-in boards (ACAO and ACJr, Strawberrysoft, Sunnyvale, CA) and triggering an ESR spectrometer (ESP 300E, Bruker, Karlsruhe, Germany) as well as a 1024 diode array UV−visible spectrometer (INSTASPEC II, LOT Oriel, Darmstadt, Germany) as reported (in an earlier paper[38]).

The UV−vis spectrometer was used in the kinetic mode with external trigger using an integration time of 80 ms. The 75 W Xe lamp as a light source and the spectrometer were connected by optical waveguides to the modified optical ESR cavity ER4104OR (Bruker, Karlsruhe, Germany) resonant in the TE_{102} mode with its special adapters for this application.[38]

As a reference electrode, a silver chloride coated silver wire in the same electrolyte was used for the spectroelectrochemical measurement and fixed in a thin flexible Teflon tube (outer diameter of less than 300 μm).

Outside the electrochemical flat cell a glass capillary filled with magnesium oxide powder containing traces of Mn^{2+} was fixed. This Mn^{2+} sample was calibrated with a Strong Pitch sample (Varian) in a double rectangular cavity ER4105DR (Bruker, Karlsruhe, Germany) to determine the absolute numbers of the electrochemically generated spins in the polymer layer.

Under the same conditions an ESR spectrum was recorded as a reference spectrum to separate the ESR signal of the polymer layer from the signal of the manganese sample.

2.2. Preparation of the Laminated Gold Micromesh Electrodes. Commercially available thermal lamination foils (laminating pouches DOCUSEAL 100 μm/5 mil, General Binding Corporation, Northbrook, IL) of different thicknesses have been shown to be resistant against solvents such as acetonitrile (AN), dimethyl sulfoxide (DMSO), dimethylformamide (DMF), and others that are frequently used for electrochemical investigations. The lamination technique is applied to give gold micromeshes a sufficient mechanical stability. In this

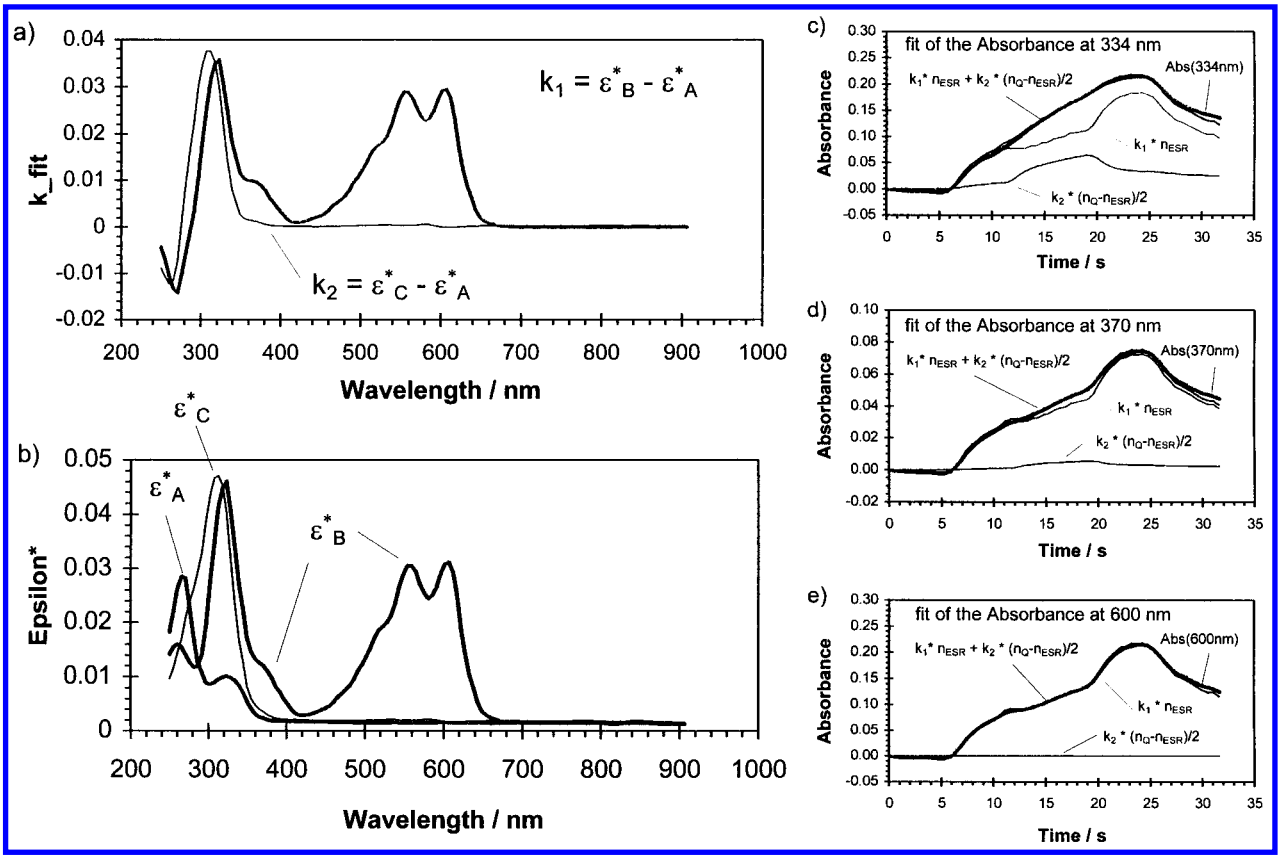

Figure 2. Separation of the superimposed UV−vis spectra of the spectroelectrochemical measurement shown in Figure 1: (a) results of the linear regression corresponding to eqs 2 and 3 with $k_1(\lambda) = \epsilon_B(\lambda) - \epsilon_A(\lambda)$, $k_2(\lambda) = \epsilon_C(\lambda) - \epsilon_B(\lambda)$ and $\epsilon = \text{abs}_i/n_i$; (b) deconvoluted spectra of the starting material A, the radical cation B, and the dication C and examples of fits of the absorbance−time dependence of the charge and the ESR intensity at different wavelengths to evaluate the $k_1(\lambda) = \epsilon_B(\lambda) - \epsilon_A(\lambda)$ and $k_2(\lambda) = \epsilon_C(\lambda) - \epsilon_B(\lambda)$; (c) at 334 nm where the radical cation as well the dication shows a strong absorption; (d) at 370 nm where the absorbance of the radical is superimposed on the absorbance band of the dication and the starting material; (e) at 600 nm where only the radical cation absorbs.

state they can be handled as optical transparent electrodes with insulated edges.[39]

By thermal lamination of the gold micromesh (gold mesh LS148120 B G, Goodfellow Ltd., Cambridge, U.K.) between two laminating foils with holes for the active electrode surface, such meshes can be mechanically stabilized, insulated, and connected with a wire to have an insulated electrical contact to the well-defined working electrode. The lamination procedure and the properties of the so-prepared optically transparent electrodes are described in ref 39.

2.3. Chemicals, Solution, and Preparation Conditions of the PAni Layer. Acetonitrile (AN) and sulfuric acid were used as purchased (analytical grade, Fluka). Water was twice-distilled before use. Solutions were prepared under inert conditions. The solvent reservoir bottle and test tubes (all equipped with septa) were connected directly via stainless steel transfer needles. The inert gas (nitrogen, pressure $p < 0.5$ bar) was used to deaerate and to transfer the solutions from the reservoir of the solvent over the molecular sieve to 4 mL special test tubes to prepare the solution and transfer it via a flexible Teflon tube into the spectroelectrochemical flat cell containing the laminated gold micromesh working electrode.

To avoid changes in the polymer deposition caused by finite diffusion conditions, the polyaniline layers on the Au-μ-mesh were electrochemically prepared in a standard electrochemical cell outside the spectroelectrochemical cell. The electropolymerization was carried out in a 70 mM solution of aniline in 1 M sulfuric acid in a mixture of acetonitrile and twice-distilled water in a ratio of 1:1, cycling the potential range from 0 to 0.850 mV vs SCE and one initial scan from 0 to 1000 mV. The polymerization was stopped after 15 cycles. These standard conditions were already used in former investigations of electrochemically prepared PAni layers.[40] The thickness of the PAni layer was estimated after the experiments under the microscope by comparing the coated mesh with an uncoated one. A thickness of the carefully dried PAni layer was estimated to be 0.25 μm, whereas the images of the Au-μ-mesh with a PAni layer after removal from the electrolyte clearly show that the 11 μm × 11 μm meshes are completely filled with polymer swelled in the solvents.

The solvents (used for the reference experiment to prove the separation procedure) acetonitrile, AN (0.005% residual water), and the supporting electrolyte tetrabutylammonium hexafluorophosphate, Bu_4NPF_6 (electrochemical grade), were purchased from Fluka and used without further purification.

Wurster Reagent WR (*N*,*N*,*N*′,*N*′-tetramethyl-1,4-phenylenediamine) from Fluka was purified by vacuum sublimation before use.

3. Results and Discussion

3.1. Separation of Superimposed Spectra by Analysis of the Time Dependence of the Absorbance, the Charge, and the ESR Intensity. The absorption bands of the starting material and the electrochemically generated products are often not well separated, which does not allow us to get reliable kinetic information from traces at the selected wavelength. The problem can be solved for electrochemical experiments in solution by use of capillary slit cells with fast conversion times[41,42] where

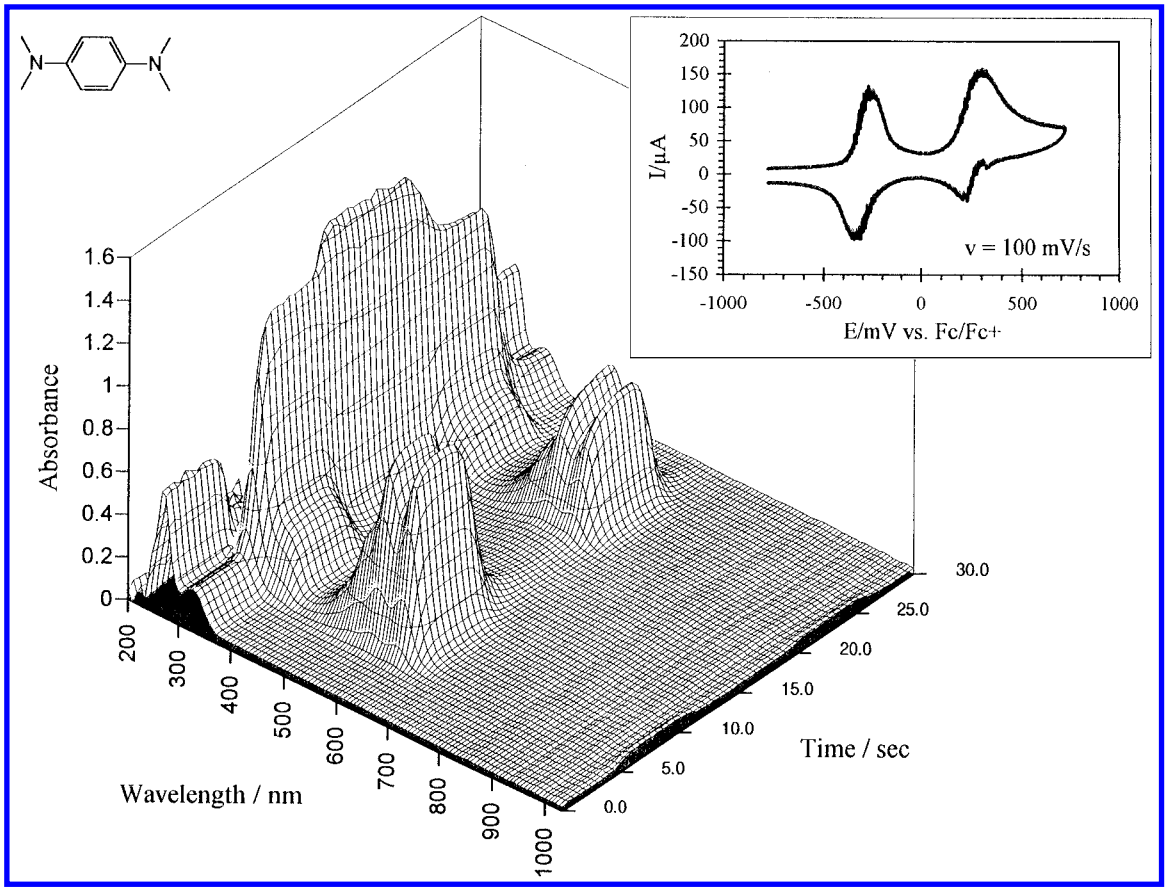

Figure 3. UV−vis spectrocyclovoltammogram of a solution of 3.81 mM Wurster reagent (0.2 M Bu_4NPF_6) under thin-layer conditions using a gold LIGA structure with a structure height of 100 μm as working electrode in a capillary slit width of 150 μm between two quartz rods[41,42] recorded at 100mV/s.

the spectra of different species can directly be obtained in the different potential/time regions. In the case of fast chemical processes or if the formal potentials are not well separated or inverted, the UV−vis spectrum of each single component is not available even under capillary slit conditions of the electrochemical cell.

The spectroelectrochemical behavior of conductive polymer films gives information on the band energies of neutral, polaronic, and bipolaronic as well as transversal polaronic states, but the situation starts to become more difficult because of the broad absorption bands of such materials. The band energies derived from UV−vis spectroelectrochemical experiments are mostly approximations that include tremendous error, and an error analysis cannot be done from only the spectroscopic data. It needs precise electrochemical current data and additional data from an independent spectroscopic method. That is why we focus on a combination of UV−vis and ESR spectroelectrochemistry done simultaneously. This method permits us not only to assign the UV−vis spectrum to a radical ion or polaronic state but also to open new possibilities of getting the individual spectra of each intermediate.

In an earlier paper[39] it was shown that laminated gold micromeshes fulfill the condition for getting precise cyclovoltammetric data in a flat cell, which can be used for UV−vis and ESR spectroscopy as well. For single electron-transfer reactions the absorbance, ESR intensity, and charge show the same time dependence as was shown for the single electron transfer to the Wurster reagent/Wurster's blue redox system.[38] Therefore, the time dependencies of the charge and the ESR intensity can be used to analyze the absorbance time dependence at selected wavelength or with the whole spectum for more complex reactions.

The most interesting case with a view on conducting polymers is a study of a two-electron transfer where the formal potentials are very close or inverted in solution.

$$A \rightleftharpoons B + e \qquad E_1^\circ, E_1^\circ > E_2^\circ$$

$$B \rightleftharpoons C + e \qquad E_2^\circ$$

$$2B \rightleftharpoons A + C \qquad K_{disp} = e^{-F(E^0{}_2 - E^0{}_1)/(RT)}$$

Under these conditions the time/potential dependence of B and C can be directly determined from the charge $Q(t)$ and the normalized ESR intensity $S_{ESR}(t)$ by $n_B(t) = S_{ESR}(t)/\epsilon_{ESR}$ where $n_B(t)$ is the amount of B at time t and $1/\epsilon_{ESR}$ is a proportionality factor determined by calibration. The amount of C at time t can be calculated with $n_C(t) = (Q(t)/F - S_{ESR}(t)/\epsilon_{ESR})/2$ where F is the Faraday constant. A secondary standard sample fixed on the electrochemical flat cell was used to determine ϵ_{ESR}, as was shown in ref 43.

An example for the simultaneous recording of ESR intensity and of the UV−vis spectra during one cyclovoltammetric scan and the determination of the time/potential dependence of the amount of substances of the starting material, the radical ion, and the dication are shown in Figure 1. The time dependence of the absorbance at one wavelength under these conditions can be written as

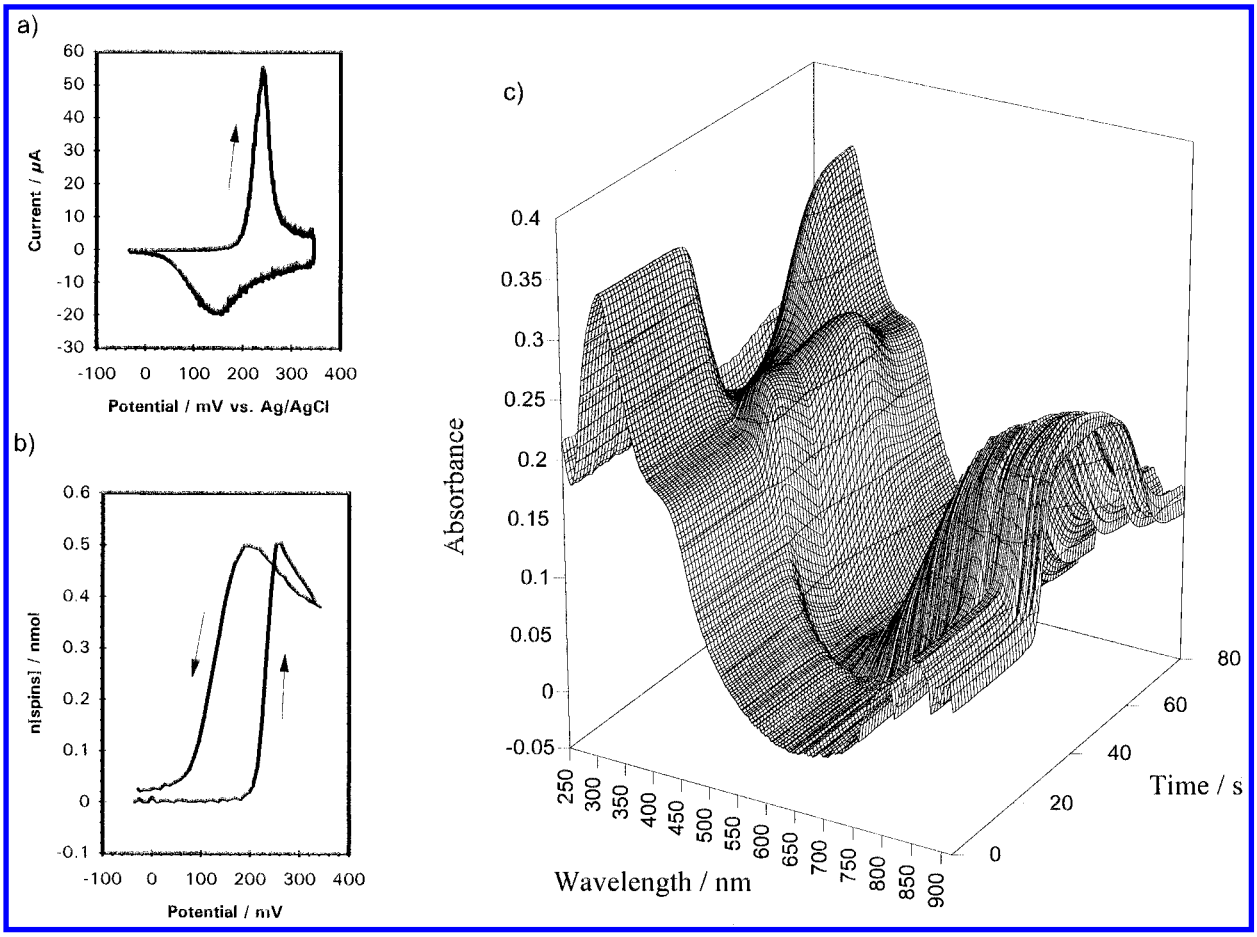

Figure 4. ESR UV−vis spectrocyclovoltammogram of a PAni layer on a laminated Au micromesh (0.86 mm × 4.19 mm) in a quartz glass flat cell in 0.1 M H_2SO_4 (H_2O/ACN = 1:1) with a slit width of 0.5 mm with 81 equidistant triggered UV−vis spectra and ESR intensity at constant field (3461 G) and a modulation amplitude of 10 G: (a) cyclovoltammetric curve with a scan rate of 10 mV/s (the background curve was recorded without polymeric layer under the same conditions); (b) ESR intensity normalized to the number of spins (the normalization was done in the same way as described earlier in ref 43); (c) UV−vis spectra recorded during the voltammetric scan.

and with $\epsilon_A = \mathrm{abs}(0)/n^\circ$ (where n° is the total number of polymer segments), it yields

$$\mathrm{abs}(t) - \mathrm{abs}(0) = \Delta\mathrm{abs}(t) = (\epsilon_B - \epsilon_A)n_B(t) + (\epsilon_C - \epsilon_A)n_C(t) \quad (2)$$

which can be written as

$$\Delta\mathrm{abs}(t) = k_1 n_B(t) + k_2 n_C(t) \quad (3)$$

The constants k_1 and k_2 can be determined by a two-dimensionallinear regression analysis, which yields the equation system

$$\begin{pmatrix} \sum_{i=1}^{n} n_{B,i} n_{B,i} & \sum_{i=1}^{n} n_{B,i} n_{C,i} \\ \sum_{i=1}^{n} n_{B,i} n_{C,i} & \sum_{i=1}^{n} n_{C,i} n_{C,i} \end{pmatrix} \begin{pmatrix} k_1 \\ k_2 \end{pmatrix} = \begin{pmatrix} \sum_{i=1}^{n} n_{B,i} \Delta\mathrm{abs}_i \\ \sum_{i=1}^{n} n_{C,i} \Delta\mathrm{abs}_i \end{pmatrix} \quad (4)$$

with

$$\det = \sum_{i=1}^{n} n_{B,i} n_{B,i} \sum_{i=1}^{n} n_{C,i} n_{C,i} - \sum_{i=1}^{n} n_{B,i} n_{C,i} \sum_{i=1}^{n} n_{B,i} n_{C,i}$$

and the solutions for

$$k_1 = \frac{\sum_{i=1}^{n} n_{B,i} \Delta\mathrm{abs}_i \sum_{i=1}^{n} n_{C,i} n_{C,i} + \sum_{i=1}^{n} n_{C,i} \Delta\mathrm{abs}_i \sum_{i=1}^{n} n_{B,i} n_{C,i}}{\det} \quad (5)$$

$$k_2 = \frac{\sum_{i=1}^{n} n_{B,i} n_{B,i} \sum_{i-1}^{n} n_{C,i} \Delta\mathrm{abs}_i - \sum_{i=1}^{n} n_{B,i} n_{C,i} \sum_{i=1}^{n} n_{B,i} \Delta\mathrm{abs}_i}{\det} \quad (6)$$

The k values can be determined at each wavelength, which allows the determination of the relative absorbance coefficients $\tilde{\epsilon}$ of each species,

$$\tilde{\epsilon}_A = \frac{\mathrm{abs}(0)}{n^\circ}$$

$$\tilde{\epsilon}_B = k_1 + \tilde{\epsilon}_A$$

$$\tilde{\epsilon}_C = k_2 + \tilde{\epsilon}_A$$

which are shown for an example in Figure 2.

The initial amount of substance n° in the capillary slit can be estimated from the volume in front of the laminated electrode

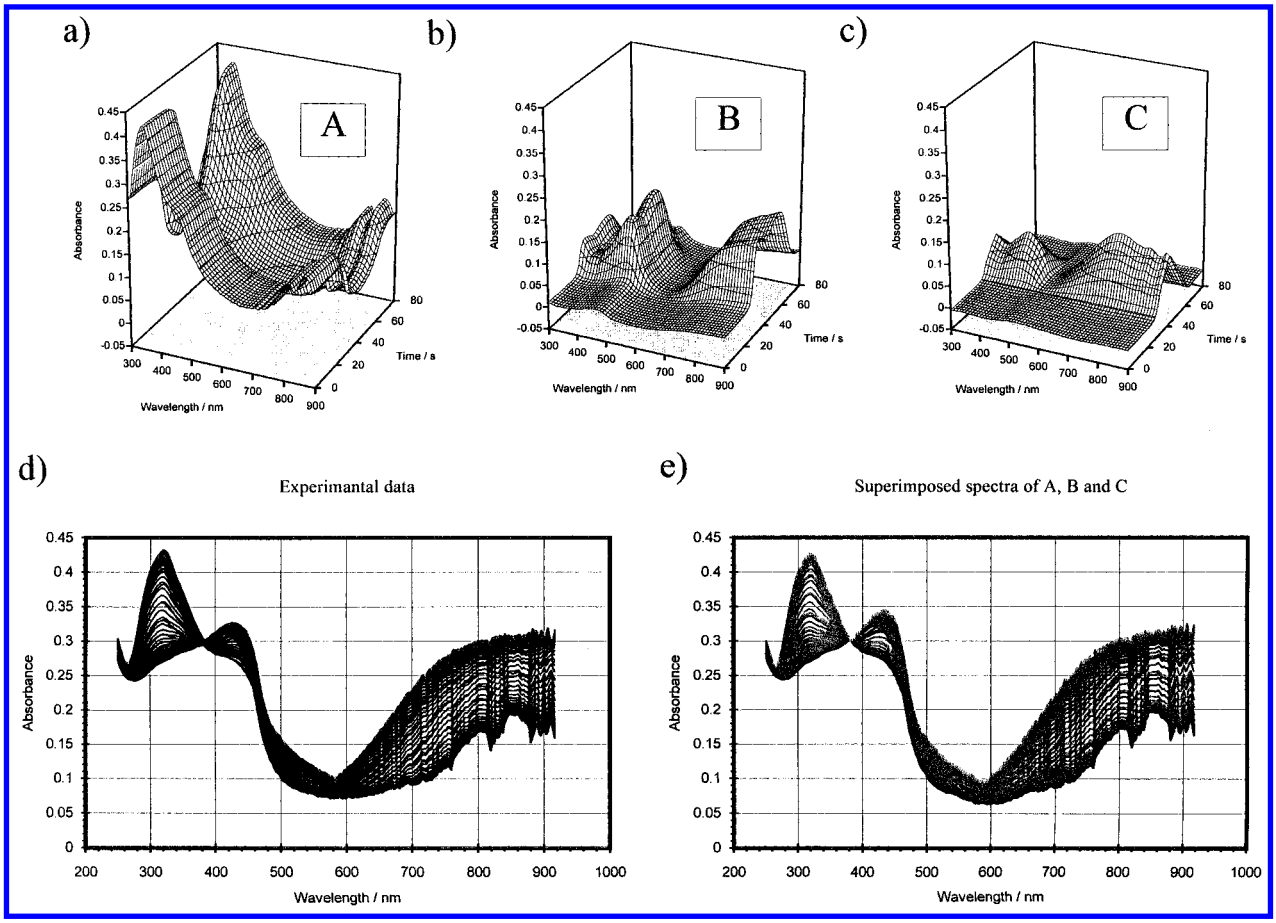

Figure 5. Time/potential dependence of the separated spectra (a) of the oxidation state A, (b) of the oxidation state B, and (c) of the oxidation state C obtained from the measurement shown in Figure 4. Also shown are (d) a 2D plot of the experimental UV−vis spectra and (e) a 2D plot of the sum of the separated spectra of the redox states A−C from parts a−c of Figure 5.

$$\mathrm{abs}(t) = \epsilon_A n_A(t) + \epsilon_B n_B(t) + \epsilon_C n_C(t) \quad (1)$$

(in the case of the measurements in Figures 1 and 2, $V = 1$ mm $\times$ 3.5 mm $\times$ 0.5 mm $= 1.75$ mm$^3 = 1.75 \times 10^{-6}$ L and the initial concentration $c^\circ = 6.1$ mM, which leads to $n^\circ = 10.7$ nmol) or, in the case of close formal potentials of the first and the second electron transfer, calculated by use of the comproportionation equilibrium

$$K_{comp} = \frac{1}{K_{disp}} = \frac{n_B(t)^2}{n_A(t) n_C(t)} \quad (7)$$

and the condition $n_A(t) + n_B(t) + n_C(t) = n^\circ$. Both yield the relation

$$\frac{n_B(t)^2}{n_C(t)} = K_{comp} n^\circ - K_{comp}(n_B(t) + n_C(t)) \quad (8)$$

which enables us to determine K_{comp} and n° from the slope and the intercept of the linear plot of

$$\frac{n_B(t)^2}{n_C(t)} \quad \text{vs} \quad (n_B(t) + n_C(t)) \quad (9)$$

The example of Wurster reagent was selected to prove the separation procedure. In the case of Wurster reagent, the second electron transfer is well separated and the separation of the spectra can be done by use of a capillary slit cell with a slit width less than 50 μm and scan rates in the range 20−100 mV/s (cf. Figure 3). The separated spectra of Figure 2 are in very good agreement with measurement results under thin-layer conditions.[41,42]

3.2. Analysis of the Time Dependence of the Absorbance Curves of ESR UV−Visible Spectrocyclovoltammograms. To study the electrochemical redox process of conducting polymer layers, the laminated gold micromesh was coated with a PAni layer. Microscopic images showed that the mesh holes were covered with PAni, which swells under the used conditions in a mixture of acetonitrile and water.

First, it was to be proved that the time dependence of the absorbance can be described by a linear combination of the ESR signal and the charge as for the mechanism I,

$$\Delta\mathrm{abs}(t) = \frac{2\epsilon_{ESR}\epsilon_B - \epsilon_C + \epsilon_A(1 - 2\epsilon_{ESR})}{2\epsilon_{ESR}} S_{ESR}(t) + \frac{\epsilon_C - \epsilon_A}{2F} Q(t)$$

$$\Delta\mathrm{abs}(t) = k_{ESR} S_{ESR}(t) + k_Q Q(t)$$

as well as for the mechanisms II and III with different constants for k_{ESR} and k_Q. Figure 4 shows the ESR UV−vis spectrocyclovoltammogram of the PAni layer.

The application of the described analysis of the time dependence of the absorbance by the ESR intensity and the

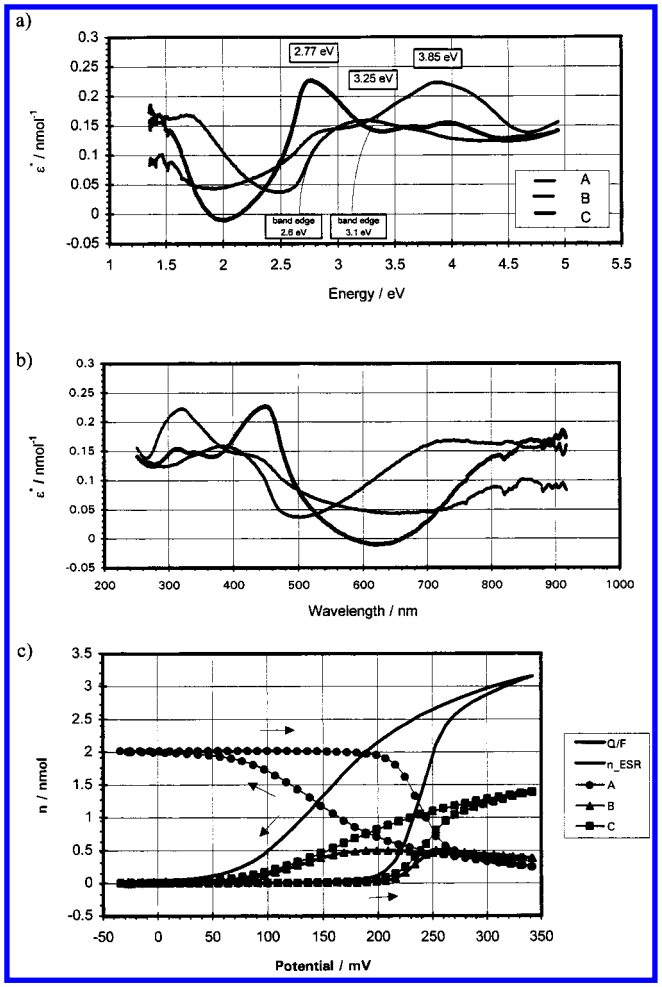

Figure 6. Spectra of the redox state of the protonated reduced PAni layer A, the polaronic deprotonated PAni layer B, and the bipolaronic state C plotted vs (a) the energy of the absorbed light and (b) the wavelength and (c) the corresponding amount of each redox state plotted vs the potential obtained by the described deconvolution procedure using the ESR intensity, the charge, and the simultaneously recorded UV−vis spectra.

charge shows that the time dependence of the absorbance at each wavelength can be described as a linear combination of the ESR intensity and the charge, as is shown in Figure 5. Thus, the determination of the separated spectra of three oxidation states and of the potential/time dependence of the three oxidation states (Figure 6) is possible.

The influence of inhomogeneous concentration dispersion in the meshes as well as incompletely covered meshes can be neglected, since it was proved by correction of the absorbance curves by the mesh effect.[43] The best fit of the time dependence of the absorbance by that of the charge and the ESR signal occurs without correction. This means that the meshes are completely covered by a swollen polymer layer and that the scan rate was slow enough to have no concentration gradient of the redox states inside the mesh holes.

4. Conclusion

The simultaneous use of ESR and UV−vis spectroscopy in cyclovoltammetric measurements enables a separation of superimposed UV−vis spectra of the electrochemically generated species, and the resulting separated UV−vis spectra can be clearly assigned to intermediates with unpaired spin and the other involved species even under semiinfinite diffusion conditions where the involved species are not resolved on the time scale of the experiments, as was shown by comparison with the results obtained under thin-layer conditions. The technique can also successfully be applied to the study of the mechanism of the redox behavior of conducting polymer layers.

The UV−vis spectra recorded during cyclic voltammetric experiments in the potential range of the first oxidation wave can be described by three components A, B, and C. The hypsochromic shift in the range 600−750 nm of the UV−vis spectra observed by other authors[44] results from the superimposed UV−vis spectra of the oxidation states B and C and not from continuous changes of the band energies during the electrochemical oxidation of the layer. If one consider the redox state B as a polaronic state and C as a bipolaronic state corresponding to mechanism I, the bipolaronic state is energetically favored and the difference of the free energy of formation of the redox states B and C can be determined from the analysis of the potential dependence of the redox states A, B, and C in the potential range close to the switching potential and yields a comproportionation constant of $K_{comp} = 0.23$ ($K_{disp} = 4.3$). That means the equilibrium is slightly shifted to the disproportionation, which means that the formal potentials are "inverted" ($E_2^0 < E_1^0$) by about 30−50 mV. But the PAni chains are deprotonated simultaneously with the electrochemical oxidation. That means the deprotonated polaronic state can be more easily oxidized than the starting material. This has to be taken into account in the discussion of the electronic structure of the redox states. The decision of whether interchain bipolaronic states (the analogues to dimers of radical ions of oligomers) are involved

cannot be made without the study of the temperature dependence of the redox process.

However, the separation of the superimposed oxidation states permits the characterization of the reduced diamagnetic initial state A by a characteristic absorption maximum at 319 nm (3.9 eV), the paramagnetic polaronic/radicalic state B by an absorption maximum at 447 nm (2.77 eV), and the third diamagnetic redox state C by an absorption at 382 nm (3.25 eV) with an onset at 2.6 eV.

Acknowledgment. The authors gratefully acknowledge grants from the Deutsche Forschungsgemeinschaft (SFB 287). We also thank Prof. G. Paasch (IFW Dresden) for discussions.

References and Notes

(1) Dunsch, L. *J. Electroanal. Chem.* **1975**, *61*, 61−80.
(2) Genies, E. M.; Lapkowski, M. *Synth Met.* **1987**, *21*, 117−121.
(3) Tang, J.; Allendorfer, R. D.; Osteryoung, R. A. *J. Phys. Chem.* **1992**, *96*, 3531−3536.
(4) Deng, Z. P.; Stone, D. C.; Thompson, M. *Analyst* **1996**, *121*, 1341−1348.
(5) Cushman, R. J.; McManus, P. M.; Yang, S. C. *J. Electroanal. Chem.* **1986**, *291*, 335.
(6) Brédas, J. L.; Scott, J. C.; Yakushi, K.; Street, G. B. *Phys. Rev. B* **1984**, *30*, 1023.
(7) Bufler, J. Ph.D. Dissertation, University Tübingen, Germany, 1993.
(8) Hill, M. G.; Mann, R. K.; Miller, L. L.; Penneau, J. P. *J. Am. Chem. Soc.* **1992**, *114*, 2728.
(9) Hill, M. G.; Penneau, J. F.; Zinger, B.; Mann, K. R.; Miller, L. L. *Chem. Mater.* **1992**, *4*, 1106.
(10) Bäuerle, P.; Segelbacher, U.; Gaudl, K.-U.; Huttenlocher, D.; Mehring, M. *Angew. Chem.* **1993**, *105*, 125.
(11) Segelbacher, U.; Sariciftci, N. S.; Grupp, A.; Bäuerle, P.; Mehring, M. *Synth. Met.* **1993**, *55*−*57*, 4728.
(12) Audebert, P.; Hapiot, P.; Pernaut, J.-M.; Garcia, P. *J. Electroanal. Chem.* **1993**, *361*, 283.
(13) Hapiot, P.; Audebert, P.; Monnier, K.; Pernaut, J.-M.; Garcia, G. *Chem. Mater.* **1994**, *6*, 1549.
(14) Smie, A.; Heinze, J. *Angew. Chem.* **1997**, *109*, 375.
(15) Ping, Z.; Nauer, G. E.; Neugebauer, H.; Theimer, J.; Neckel, A. *Electrochim. Acta* **1997**, *42*, 1693−1700.
(16) Zhao, P.; Nauer, G. E.; Neugebauer, H.; Theimer, J. *J. Electroanal. Chem.* **1997**, *420*, 301−306.
(17) Ping, Z.; Nauer, G. E.; Neugebauer, H.; Theimer, J.; Neckel, A. *Farady Trans.* **1997**, *93*, 121−129.
(18) Moll, T.; Heinze, J. *Synth. Met.* **1993**, *55*, 1521.
(19) Dunsch, L.; Lubert, K.-H. *Electrochim. Acta* **1998**, *43*, 813−822.
(20) Rossberg, K.; Paasch, G.; Dunsch, L.; Ludwig, S. *J. Electroanal. Chem.* **1997**, *443*, 49−62.
(21) Kaufmann, F. B.; Schröder, A. H.; Engler, E. M.; Kramer, S. R.; Chambers, J. Q. *J. Am. Chem. Soc.* **1980**, *102*, 483.
(22) Daum, P.; Lenhard, J. R.; Rolison, D. R.; Murray, R. W. *J. Am. Chem. Soc.* **1980**, *102*, 4649.
(23) Daum, P.; Murray, R. W. *J. Phys. Chem.* **1981**, *85*, 389.
(24) Doblhofer, K.; Braun, K.; Lange, R. *J. Electroanal. Chem.* **1986**, *206*, 93.
(25) Heinze, J.; Bilger, R. *Ber. Bunsen-Ges. Phys. Chem.* **1993**, *97*, 502.
(26) Vorotyntsev, M. A.; Vieil, E.; Heinze, J. *Russ. J. Electrochem.* **1995**, *31*, 1027.
(27) Winkels, S.; Lohrengel, M. M. *Electrochim. Acta* **1997**, *42*, 3117.
(28) Aoki, K.; Tesuka, Y. *J. Electroanal. Chem.* **1989**, *267*, 35.
(29) Aoki, K.; Cao, J.; Hoshino, Y. *Electrochim. Acta* **1994**, *39*, 2291.
(30) Vuki, M.; Kalaji, M.; Nyholm, L.; Peter, L. M. *J. Electroanal. Chem.* **1992**, *332*, 315.
(31) Vuki, M.; Kalaji, M.; Nyholm, L.; Peter, L. M. *Synth. Met.* **1993**, *55*−*57*, 1515.
(32) Lacroix, J. C.; Kanazawa, K.; Diaz, A. F. *J. Electroanal. Chem.* **1989**, *5*, 136.
(33) Lacroix, J. C. Theses du Doctorat, Université Paris 11, Paris, 1990.
(34) Genz, O. Ph.D. Dissertation, Universität Düsseldorf, Germany, 1995.
(35) Genz, O.; Lohrengel, M. M.; Schultze, J. W. *Electrochim. Acta* **1994**, *39*, 179.
(36) Lohrengel, M. M.; Genz, O. *Ionics* **1995**, *1*, 304.
(37) Malinauskas, A. *Ber. Bunsen-Ges. Phys. Chem.* **1998**, *102*, 972−973.
(38) Petr, A.; Dunsch, L.; Neudeck, A. *J. Electroanal. Chem.* **1996**, *412*, 153.
(39) Neudeck, A.; Kress, L. *J. Electroanal. Chem.* **1997**, *437*, 141.
(40) Zimmermann-Iotschewa, A. Ph.D. Dissertation, TU-Dresden, 1997.
(41) Neudeck, A.; Dunsch, L. *J. Electroanal. Chem.* **1995**, *386*, 135.
(42) Neudeck, A.; Dunsch, L. *Electrochim. Acta* **1995**, *40*, 1422.
(43) Neudeck, A.; Petr, A.; Dunsch, L. *Synth. Met.*, submitted.
(44) Brandl, V.; Holze, R. *Ber. Bunsen-Ges. Phys. Chem.* **1997**, *101*, 251.